

Ultracold Molecules in the Ro-Vibrational Ground State

F. Lang,¹ K. Winkler,¹ C. Strauss,¹
R. Grimm,^{1,2} J. Hecker Denschlag^{1*}

¹Institut für Experimentalphysik und Zentrum für Quantenphysik,
Universität Innsbruck, A-6020 Innsbruck, Austria

²Institut für Quantenoptik und Quanteninformation
der Österreichischen Akademie der Wissenschaften, A-6020 Innsbruck, Austria

* E-mail: johannes.denschlag@uibk.ac.at

The successful production of quantum degenerate gases of *weakly bound* molecules has triggered a quest for quantum gases of *tightly bound* molecules. We report here on the first production of an ultracold gas of tightly bound Rb_2 molecules in the ro-vibrational ground state, close to quantum degeneracy. This was achieved by optically transferring weakly bound Rb_2 molecules to the absolute lowest level of the $a^3\Sigma_u^+$ potential with a transfer efficiency of about 90%. The transfer takes place in a 3D optical lattice which traps a sizeable fraction of the tightly bound molecules with a lifetime exceeding 200 ms. These results open the door for experiments with tightly bound ultracold molecules, investigations of ultracold collisions and chemistry, production of a molecular Bose-Einstein condensate (BEC), and molecular quantum optics.

Standard laser cooling techniques as developed for atoms [1] do not work for molecules due to their complex internal structure. Other pathways to cold and dense samples of molecules

are required, such as Stark deceleration [2] and sympathetic cooling [3] or association of ultracold atoms [4, 5, 6]. Association via Feshbach resonances [5, 6] has directly produced quantum degenerate or near degenerate ultracold molecular gases [7, 8, 9, 10, 11, 12, 13, 14, 15], but only in very weakly bound states with a high vibrational quantum number. Furthermore, such molecules are in general unstable when colliding with each other, particularly if they are composed of bosonic atoms. Very recently optical schemes have been developed to selectively produce cold and dense samples of deeply bound molecules in the ro-vibrational ground state [16, 17, 18, 19, 20, 21]. In parallel to work of Ni *et al.* [22], we report here the first realization of this goal. We use an optical transfer of $^{87}\text{Rb}_2$ Feshbach molecules to a single quantum level in the ro-vibrational ground state of the Rb_2 triplet potential ($a^3\Sigma_u^+$), entering the regime of an ultracold and dense ensemble of tightly bound molecules. The transfer is carried out in a single step using stimulated Raman adiabatic passage (STIRAP) [23, 17, 18, 19] with an efficiency of almost 90%, which is only technically limited. The molecules are held in a 3D optical lattice in which they exhibit a trap lifetime exceeding 200 ms, after an initial relaxation within 50 ms.

The electronic ground state of Rb_2 molecules can be described in terms of two Born-Oppenheimer potentials, $X^1\Sigma_g^+$ and $a^3\Sigma_u^+$. The corresponding singlet and triplet molecular states have different properties. Due to tighter bonding as compared to triplet states, the singlet ro-vibrational ground state is intrinsically stable when subjected to cold collisions. Molecules in the triplet ro-vibrational ground state can potentially relax to the singlet state through inelastic collisions, a process which has not yet been investigated. In contrast to singlet molecules, triplet molecules exhibit a magnetic moment giving rise to a rich energy level structure in the presence of magnetic fields. Thus collisions of triplet molecules should exhibit magnetically tunable scattering resonances, e.g., Feshbach resonances. Assuming a regime where elastic collisions dominate, this opens interesting prospects for future experiments with molecular Bose-Einstein

condensates and ultracold chemistry [24].

The starting point for our transfer experiments is a $50\mu\text{m}$ -size pure ensemble of 3×10^4 weakly bound Rb_2 Feshbach molecules which have been produced from an atomic ^{87}Rb Bose-Einstein condensate using a Feshbach resonance at a magnetic field of 1007.4 G [25], ($1\text{ G} = 10^{-4}\text{ T}$). They are trapped in the lowest Bloch band of a cubic 3D optical lattice with no more than a single molecule per lattice site [25] and an effective lattice filling factor of about 0.3. Using an optical lattice not only has advantages for the preparation, manipulation and purification of molecular ensembles [25, 17, 26], it also directly produces a quantum lattice gas of molecules with which interesting experiments can be carried out, see e.g. [27]. In our experiment, the lattice depth for the Feshbach molecules is $60 E_r$, where $E_r = \pi^2 \hbar^2 / 2ma^2$ is the recoil energy, with m the mass of the molecules and $a = 415.22\text{ nm}$ the lattice period. Such deep lattices suppress tunneling between different sites. The magnetic field is set to 1005.8 G where the Feshbach molecules are in a quantum state $|f\rangle$ which correlates with $|F = 2, m_F = 2, f_1 = 2, f_2 = 2, v_t = 37, l = 0\rangle$ at 0 G . Here, F and $f_{1,2}$ are the total angular momentum quantum numbers for the molecule and its atomic constituents, respectively, and m_F is the total magnetic quantum number; v_t is the vibrational quantum number for the triplet potential and l is the quantum number for rotation.

For the transfer we use a stimulated optical Raman transition. Two lasers (1 and 2) connect the Feshbach molecule level $|f\rangle$, via an excited level $|e\rangle$, to the absolute lowest level in the triplet potential $|g\rangle$ (see Fig. 1A). State $|g\rangle$ has a binding energy of $7.0383(2)\text{ THz} \times h$ and can be described by the quantum numbers $|F = 2, m_F = 2, S = 1, I = 1, v_t = 0, l = 0\rangle$ where S and I are the total electronic and nuclear spins of the molecule, respectively. At 1005.8 G the ground state is separated by hundreds of MHz from any other bound level, so there is no ambiguity in what level is addressed. The level $|e\rangle$ is located in the vibrational $v=13$ manifold of the electronically excited $^3\Sigma_g^+$ ($5s + 5p$) potential and has 1_g character. It has an excitation

energy of $294.6264(2)\text{ THz}\times h$ with respect to $|f\rangle$, a width $\Gamma = 2\pi \times 8\text{ MHz}$ and a Zeeman shift of $3.4\text{ MHz}\times h/G$. From resonant excitation measurements we deduce a coupling strength for the transition from $|f\rangle$ to $|e\rangle$ of $C_1 = \Omega_1/\sqrt{I_1} = 2\pi \times 0.4\text{ MHz}/\sqrt{W\text{cm}^{-2}}$ where Ω_1 is the Rabi frequency and I_1 is the intensity of laser 1. In comparison, the coupling strength for the transition from $|g\rangle$ to $|e\rangle$ is $C_2 = 2\pi \times 30\text{ MHz}/\sqrt{W\text{cm}^{-2}}$. We deduce C_2 from the measured width of a dark resonance which appears when both lasers resonantly couple to level $|e\rangle$ (see Fig. 1B). The broadening of the dark resonance depends on Ω_2 and is directly related to Autler-Townes splitting [12].

The positions of the deeply bound energy levels of the excited $^3\Sigma_g^+$ and the ground state $a\ ^3\Sigma_u^+$ Rb₂ potential are not precisely known. Therefore, we have carried out extensive single- and two-color spectroscopy on our pure ensemble of Feshbach molecules. In particular, we have mapped out the vibrational progression of both potentials to the ground state $v_t = 0$. In general, levels were identified by comparing our measured spectra and transition strengths to theoretical predictions based on *ab-initio* potentials. Especially for the levels of the $a\ ^3\Sigma_u^+$ potential where calculations are based on a close-coupled channel model, we found excellent agreement with the predicted level structure and level splittings. A detailed discussion of the measurements of the spectra as well as their analysis will be presented elsewhere.

STIRAP is a very efficient transfer method based on a stimulated Raman transition [23]. It uses a counter-intuitive pulse sequence during which molecules are kept in a dynamically changing dark superposition state $|\Psi_{ds}\rangle = (\Omega_2|f\rangle - \Omega_1|g\rangle)/\sqrt{\Omega_1^2 + \Omega_2^2}$. This dark state is decoupled from the light in the sense that there is no excitation of the short lived state $|e\rangle$, which suppresses losses during transfer. A vital condition for STIRAP is the relative phase stability between the two Raman lasers. Both of our Raman lasers, a Ti:Sapphire laser (laser 1) and a grating-stabilized diode laser (laser 2) are Pound-Drever-Hall locked to a single cavity which itself is locked to an atomic ^{87}Rb -line. From the lock error signals, we estimate frequency

stabilities on a ms-timescale of 40 kHz and 80 kHz for lasers 1 and 2, respectively. Thus, the transfer has to take place on a μs timescale in order not to lose phase coherence during STIRAP. Both laser beams have a waist of $130\ \mu\text{m}$ at the location of the molecular sample, propagate collinearly, and are polarized parallel to the direction of the magnetic bias field. Thus the lasers can only induce π transitions.

As a first step towards STIRAP, we determine important properties of our system and check for consistency. This is done by exposing $|f\rangle$ molecules to a square wave pulse of Raman laser light and observing the dynamics [for details see appendix A1]. Essentially, our system is very well described by a closed three level system (a Λ system) and its dynamics can be modeled with a master equation [see appendix A2]. Decoherence effects can be accounted for as phase fluctuations of the Raman lasers. These fluctuations can be expressed in terms of a short-term relative linewidth of the lasers, γ , which we find to be about $2\pi \times 20\text{kHz}$.

We now perform STIRAP by adiabatically ramping the Raman laser intensities instead of using square wave pulses (see right inset in Fig. 2). This efficiently transfers the molecules from $|f\rangle$ to $|g\rangle$. In order to detect the molecules in state $|g\rangle$ after the transfer, we bring them back to $|f\rangle$ with a second, reversed STIRAP pulse sequence. We then dissociate the molecules into pairs of atoms at the Feshbach resonance. By releasing these atoms from the optical lattice in the manner described in [26], we can map out the Bloch bands in momentum space. After 13 ms of ballistic expansion the corresponding atomic distribution is recorded with standard absorption imaging (see left inset in Fig. 2). For our signals, we only count atoms in the central square zone, corresponding to the lowest Bloch band[26].

Figure 2 shows the total transfer efficiency after two such STIRAP transfers which are separated by a hold time $\tau_h = 2\ \mu\text{s}$. The transfer efficiency for this *round trip STIRAP process* is plotted as a function of the two-photon detuning δ and reaches about 75% at resonance ($\delta = 0$). Assuming equal efficiencies for both transfers, this corresponds to a single transfer efficiency

of 87% and a total number of 2.6×10^4 molecules in state $|g\rangle$. The 1 MHz width (FWHM) of the transfer efficiency is determined by power- and Fourier-broadening [28] and is in good agreement with our master equation model, represented by the solid lines in Fig. 2. These calculations indicate that half of the losses are due to nonadiabaticity and half are due to the non-ideal laser system. We have experimentally verified that no molecules remain in state $|f\rangle$ between the two STIRAP pulses (blue diamonds in Fig. 2). Any such molecules would quickly be removed by laser 1 at the end of the first STIRAP pulse, which is kept on at maximum power for $1\mu\text{s}$ after ramping down laser 2. Thus, all molecules that are retrieved after the second STIRAP transfer have been deeply bound in state $|g\rangle$.

We also investigate the dynamics and lifetime of the deeply bound molecules in the optical lattice. Due to their strong binding, molecules in state $|g\rangle$ cannot be expected to have a polarizability similar to that of Feshbach molecules, and it is not clear what strength or even sign the optical lattice potential will have for them. Indeed, as we show below, the lattice potential is attractive for the $|g\rangle$ molecules, but a factor 10 ± 2 shallower compared to the potential for the Feshbach molecules. Repeating the transfer experiment, we now vary the hold time τ_h between the two STIRAP transfers (see Fig. 3). Interestingly, for short hold times the transfer efficiency exhibits a damped oscillation (see inset). The period and damping time are both about $80\mu\text{s}$. After $250\mu\text{s}$ the efficiency levels off at 40% and then decays much more slowly. The initial oscillation can be understood as follows. We consider the localized spatial wavepacket of a Feshbach molecule at a particular lattice site in the lowest Bloch band. The first STIRAP transfer projects this wavepacket onto the much shallower lattice potential felt by the $|g\rangle$ molecules. As a consequence $|g\rangle$ molecules are coherently spread over various Bloch bands, and the wavepacket undergoes “breathing” oscillations with the lattice site trap frequency ω_t . These coherent oscillations are damped by tunneling of $|g\rangle$ molecules in higher Bloch bands to neighboring lattice sites. The reverse STIRAP transfer maps this periodic oscillation back

to the Feshbach molecules. Higher Bloch bands are populated here as well, but are at most partially counted in our scheme, which leads to an apparent loss of our transfer efficiency. We can describe the data well using a 3D multi-band model (see solid blue line, inset Fig. 3). In this model the states $|f\rangle$, $|e\rangle$ and $|g\rangle$ obtain a substructure due to the Bloch bands of the optical lattice and the resulting levels are coupled by the laser fields [for details see appendix A3]. From fits to the data we extract the lattice site trap frequency ω_t , which determines the lattice depth for the molecules in state $|g\rangle$.

The question arises why similar oscillations are not observed in our dark state measurements shown in Fig. A1 [see appendix], especially for the case $\Omega_1 = \Omega_2$ where 50% of the population is in state $|g\rangle$. This behavior can be reproduced precisely with our multi-band model. In essence, strong coupling of the levels via the Raman lasers suppresses the breathing oscillations by locking the phases of the different quantum levels to each other. We note that the theoretical analysis of Fig. 2 does not include optical lattice effects. However, because the hold time τ_h is so short (2 μ s), molecule signal losses due to oscillation amount to only 4% and thus do not seriously affect the previous analysis. In fact, the multi-band model leads to the same theoretical curve as shown when we use a short-term relative laser line width $\gamma = 2\pi \times 18$ kHz, in agreement with the value from the square-pulse measurements.

For longer hold times of up to 200 ms, Figure 3 shows the time dependent loss of the deeply bound molecules. Within the first 50 ms the fraction of recovered molecules drops to 20%. We attribute this loss mainly to the fact that all molecules in excited bands will simply fall out of the lattice since they are essentially unbound. For the remaining molecules in the lowest band we find a lifetime exceeding our maximum experimental observation time which is limited due to heating of the magnetic field coils.

To conclude, using a nearly 90% efficient STIRAP transfer we have created an ultracold ensemble of deeply bound Rb_2 molecules in the absolute lowest quantum state of the $a^3\Sigma_u^+$

potential. These deeply bound molecules were trapped in a 3D optical lattice and we observed coherent motional dynamics of their spatial wavepackets in the sites. This indicates that besides the internal degrees of freedom, the external degrees of freedom are also precisely defined after transfer. The transfer of molecules into a single Bloch band should be possible, either by matching the lattice depths of weakly and deeply bound molecules, or by spectroscopically resolving the Bloch bands [31]. The latter involves longer STIRAP pulses and more tightly phase-locked Raman lasers, with the added benefit of increasing the transfer efficiency further. Investigating the collisional behavior of the triplet molecules will be the next goal as it is of central importance for ultracold chemistry [24] and for achieving molecular BEC. An appealing way to reach BEC is by melting an optical-lattice-induced Mott insulator of ro-vibrational ground state molecules [27]. For this, we have to improve the lattice occupation of our initial ensemble of Feshbach molecules [13] and use a selective STIRAP transfer to the lowest Bloch band.

The authors thank Christiane Koch, Eberhard Tiemann, Olivier Dulieu, Paul Julienne and Roman Krems for valuable discussions and information material such as transition matrix elements and molecular bound state tables. We are indebted to Paul Julienne for furnishing us with a numerical code from NIST to calculate molecular bound state levels and we thank Peter v.d. Straten and Birgit Brandstätter for setting it up. We thank Helmut Ritsch for very helpful discussions and support in model calculations. We also thank Gregor Thalhammer, Devang Naik, Tetsu Takekoshi for assistance in the lab, the team of Hanns-Christoph Nägerl for helpful exchange, and Florian Schreck for loaning us a Verdi V18 pump laser. This work was supported by the Austrian Science Fund (FWF) within SFB 15 (project part 17).

References and Notes

- [1] H. J. Metcalf, P. van der Straten, *Laser Cooling and Trapping* (Springer-Verlag, New York, 1999).
- [2] S. Y. T. van de Meerakker, H. L. Bethlem, G. Meijer, *Nature Physics* **4**, 595 - 602 (2008).
- [3] J. Doyle, B. Friedrich, R. V. Krems, F. Masnou-Seeuws, *Eur. Phys. J. D* **31**, 149-164 (2004).
- [4] K. M. Jones, E. Tiesinga, P. D. Lett, P. S. Julienne, *Rev. Mod. Phys.* **78**, 483-535 (2006).
- [5] T. Köhler, K. Goral, P. S. Julienne, *Rev. Mod. Phys.* **78**, 1311-1361 (2006).
- [6] J. M. Hutson, P. Soldán, *Int. Rev. Phys. Chem.* **25**, 497-526 (2006).
- [7] J. Herbig *et al.*, *Science* **301**, 1510 - 1513 (2003).
- [8] K. Xu *et al.*, *Phys. Rev. Lett.* **91**, 210402 (2003).
- [9] S. Jochim *et al.*, *Science* **302**, 2101-2103 (2003).
- [10] M. Greiner, C. A. Regal, D. S. Jin, *Nature* **426**, 537-540 (2003).
- [11] M. W. Zwierlein *et al.*, *Phys. Rev. Lett.* **91**, 250401 (2003).
- [12] K. Winkler *et al.*, *Phys. Rev. Lett.* **95**, 063202 (2005).
- [13] T. Volz *et al.*, *Nature Physics* **2**, 692-695 (2006).
- [14] T. Bourdel *et al.*, *Phys. Rev. Lett.* **93**, 050401 (2004).
- [15] G. B. Partridge, K. E. Strecker, R. I. Kamar, M. W. Jack, R. G. Hulet, *Phys. Rev. Lett.* **95**, 020404 (2005).

- [16] J. M. Sage, S. Sainis, T. Bergeman, D. DeMille, *Phys. Rev. Lett.* **94**, 203001 (2005).
- [17] K. Winkler *et al.*, *Phys. Rev. Lett.* **98**, 043201 (2007).
- [18] S. Ospelkaus *et al.*, *Nature Physics* **4**, 622-626 (2008).
- [19] J. G. Danzl *et al.*, *Science*, **321** 1062-1066 (2008). Published online 10 July 2008 (10.1126/science.1159909).
- [20] M. Viteau *et al.*, *Science* **321**, 232 (2008).
- [21] J. Deiglmayr *et al.*, preprint, arxiv:08073272v1 (2008)
- [22] K.-K. Ni *et al.*, preprint, arXiv:0808.2963 (2008).
- [23] K. Bergmann, H. Theuer, B. W. Shore, *Rev. Mod. Phys.* **70**, 1003-1025 (1998).
- [24] R. V. Krems, *Phys. Chem. Chem. Phys.* **10**, 4079-4092 (2008).
- [25] G. Thalhammer *et al.*, *Phys. Rev. Lett.* **96**, 050402 (2006).
- [26] K. Winkler *et al.*, *Nature* **441**, 853-856 (2006).
- [27] D. Jaksch, V. Venturi, J.I. Cirac, C. Williams, P. Zoller, *Phys. Rev. Lett.* **89**, 040402 (2002).
- [28] The actual population transfer in each STIRAP pulse takes place in $2\mu\text{s}$.
- [29] D. F. Walls, G. J. Milburn, *Quantum Optics* (Springer-Verlag, Berlin, 1994).
- [30] T. Haslwanter, H. Ritsch, J. Cooper, and P. Zoller, *Phys. Rev. A* **38**, 5652-5659 (1988).
- [31] T. Rom *et al.*, *Phys. Rev. Lett.* **93**, 073002 (2004).

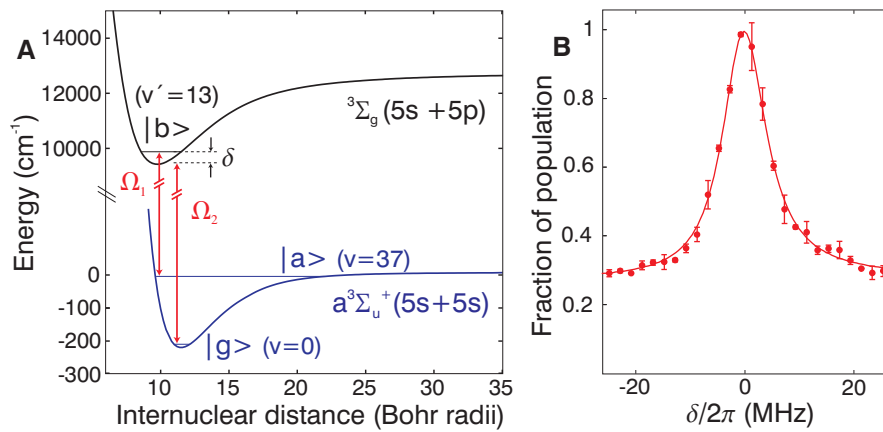


Figure 1: **A** Molecular levels of Rb₂. The lasers 1 and 2 couple the molecule levels $|f\rangle$, $|g\rangle$ to the excited level $|e\rangle$ with Rabi frequencies $\Omega_{1,2}$, respectively. Note the different energy scales for the electronic ground and excited molecular potentials. **B** Dark resonance. The data shows the remaining fraction of Feshbach molecules $|f\rangle$ after exposing them to both Raman lasers in a $3\mu\text{s}$ square pulse. The two photon detuning δ is scanned by varying the wavelength of laser 2 while keeping laser 1 on resonance. The Rabi frequencies are $\Omega_1 = 2\pi \times 0.7$ MHz and $\Omega_2 = 2\pi \times 10$ MHz. The solid line is a fit from a simple three level model [17].

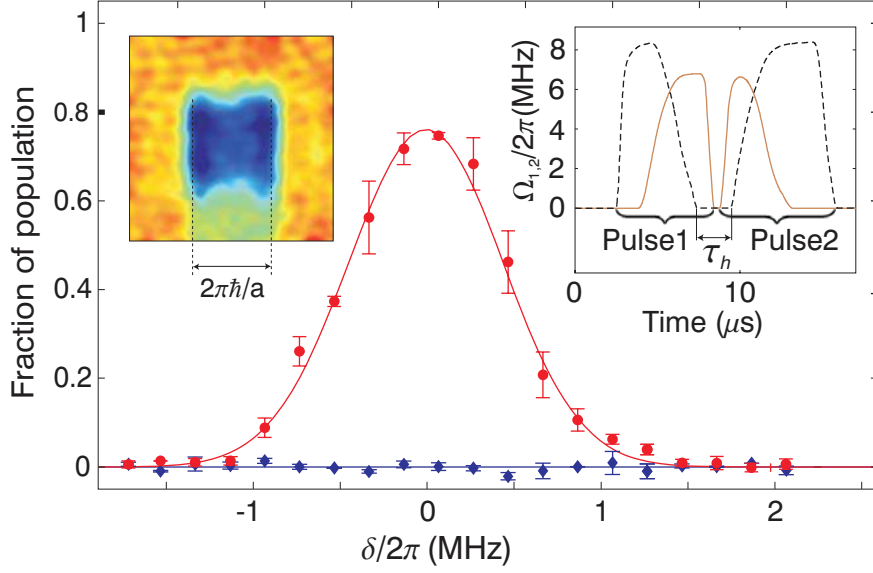


Figure 2: STIRAP. We plot the efficiency for population transfer from state $|f\rangle$ to state $|g\rangle$ and back with two STIRAP pulses (red circles) as a function of two photon detuning δ , reaching a maximum of 75%. In the dead time between the two STIRAP pulses, no Feshbach molecules can be detected (blue diamonds). The continuous lines are from model calculations as described in the text. The right inset shows the corresponding pulse sequence indicating the Rabi frequencies of laser 1 (solid brown line) and laser 2 (dashed black line). The hold time τ_h , the time between the actual population transfers, is equal to $2\mu\text{s}$. The left inset is a false-color absorption image which displays the atomic quasi-momentum distribution in the optical lattice after the round-trip STIRAP transfer and subsequent adiabatic molecule dissociation. Atoms located in the inner square stem from the lowest Bloch band. $2\pi\hbar/a$ is the modulus of reciprocal lattice vector.

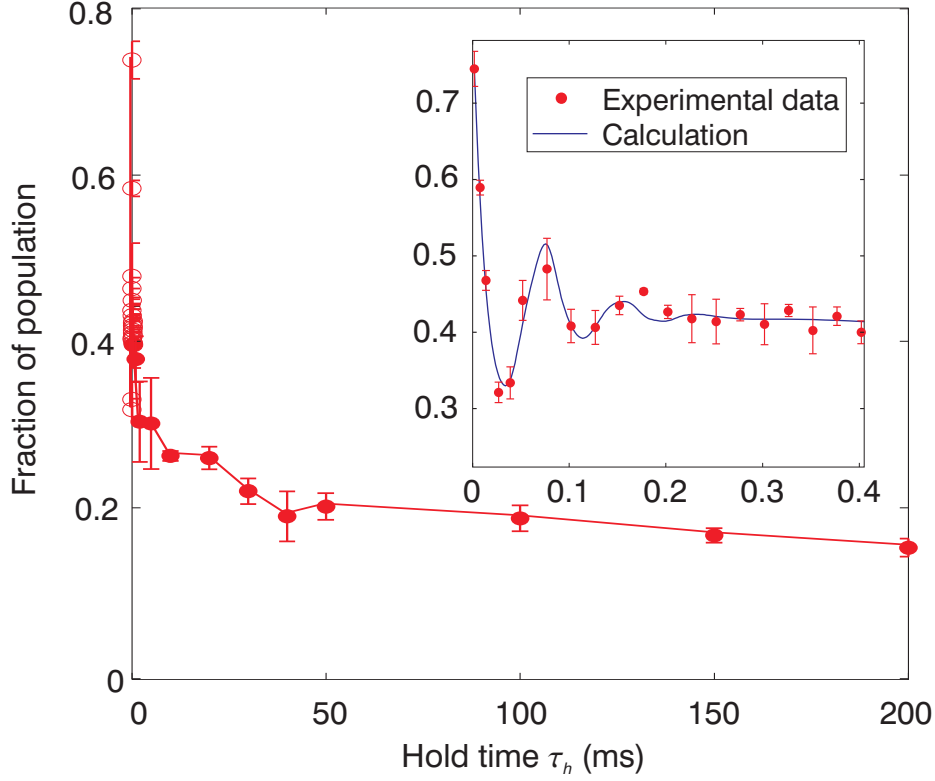


Figure 3: Dynamics and lifetime of $|g\rangle$ molecules in the optical lattice. We plot the transfer efficiency for the round trip STIRAP process as a function of the hold time τ_h between the two STIRAP pulses. We only count molecules whose constituent atoms end up in the lowest Bloch band after transfer (see left inset of Fig. 2). Except for τ_h , all other experimental parameters are the same as in Fig. 2. Molecules are lost on three different timescales, $100\mu\text{s}$, 50ms , and $\approx 200\text{ms}$. The inset zooms into the first $400\mu\text{s}$. The oscillations in the transfer efficiency are due to breathing oscillations of localized spatial wavepackets of molecules in the lattice sites. The solid blue line is from a multi-band model calculation [see appendix]. The data shown in the inset are plotted with open plot symbols in the main plot. The line connects neighboring data points.

Appendix

A1. Raman Square Pulse Measurements

We can determine important properties of our Raman transfer system by exposing the Feshbach molecules $|f\rangle$ simultaneously to a square pulse of Raman lasers 1 and 2. Figure 4 shows the remaining fraction of molecules in state $|f\rangle$ after a variable pulse time. Within $1\ \mu\text{s}$ we observe a rapid loss of molecules that depends on the ratio Ω_2/Ω_1 . The remaining molecules are stable on a much longer timescale. This can be understood in terms of formation of a dark state $|\Psi_{ds}\rangle$. In fact, we can write $|f\rangle = (\Omega_2|\Psi_{ds}\rangle + \Omega_1|\Psi_{bs}\rangle)/\sqrt{\Omega_1^2 + \Omega_2^2}$ where $|\Psi_{bs}\rangle$ is a bright state which quickly decays via excitation of level $|e\rangle$. The dark state remains and can be detected as a fraction $\Omega_2^4/(\Omega_1^2 + \Omega_2^2)^2$ of remaining molecules in $|f\rangle$. We use this fact to calibrate

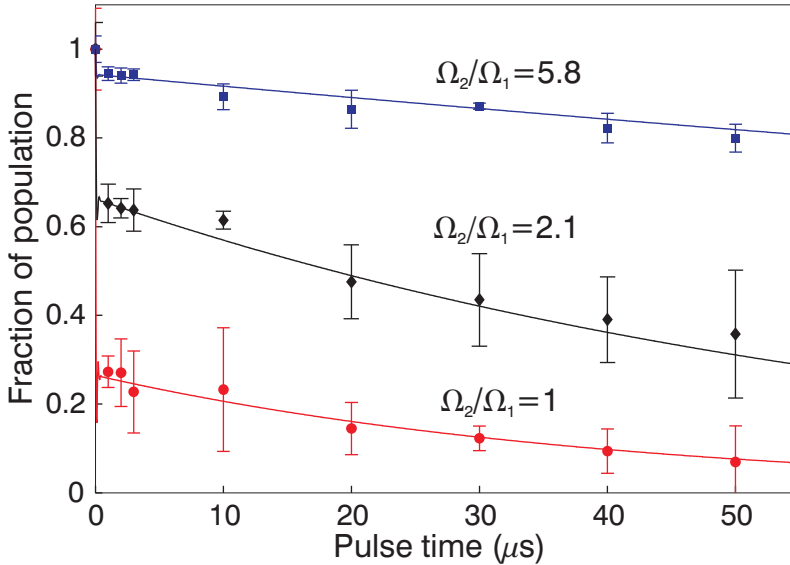


Figure 4: Dark state formation and lifetime. Shown is the fraction of remaining Feshbach molecules after subjecting them to a square pulse of Raman laser light with variable time length for various ratios of Rabi frequencies Ω_2/Ω_1 ($\Omega_2 \approx 2\pi \times 7\ \text{MHz}$). After switching on the lasers, a certain fraction of molecules is lost within $1\ \mu\text{s}$ and a dark state has formed which has a much longer lifetime. The solid lines represent model calculations (see section A2) which can be used to determine the Rabi frequencies and short-term laser line widths.

the Rabi frequency ratio Ω_1/Ω_2 and find good agreement with our previously discussed calibration methods. A fraction $\Omega_1^2\Omega_2^2/(\Omega_1^2 + \Omega_2^2)^2$ of the initial molecules is in state $|g\rangle$ and has a maximum of 25% for $\Omega_1 = \Omega_2$. Thus, a sizeable fraction of the molecules can be coherently transferred to the ground state $|g\rangle$ by simply switching on both Raman lasers. Remarkably, this transfer takes place in less than 1 μs .

As can be seen from Fig. 4, the dark state slowly decays. Its lifetime is shortest for $\Omega_1 = \Omega_2$, where we measure it to be $\approx 50 \mu\text{s}$. The decay of the dark state is likely due to phase fluctuations of the Raman lasers. In principle, the decay of the dark state could have contributions due to other effects, as for example, coupling to levels outside of $|f\rangle$, $|e\rangle$, and $|g\rangle$. However, we have verified that this is not the case, because losses due to optical excitation are completely negligible when we expose a pure ensemble of $|f\rangle$ ($|g\rangle$) molecules only to laser 2 (1). We can describe all data in Fig. 4 very well with a master equation model (see section A2). It takes into account the previously determined linewidth Γ of the excited level, detuning δ and Rabi frequencies $\Omega_{1,2}$. It leaves the short-term relative linewidth of both lasers, γ , as a fit parameter which we determine to be about $2\pi \times 20 \text{ kHz}$.

In another set of experiments, we searched for laser power dependent shifts of the two-photon Raman resonance. Using the Raman square pulse measurements, we scanned the relative detuning of the lasers for a fixed pulse time and various laser powers. Within the accuracy of our measurements of $2\pi \times 200 \text{ kHz}$ we could not detect any laser power dependent shifts of the two-photon resonance.

A2. Master equation

Neglecting lattice effects, we can describe the internal dynamics of the molecules as they are subjected to the Raman laser fields with a 3-level model. We use a master equation (see references [29, 30]) which takes into account decoherence due to phase fluctuations of the Raman

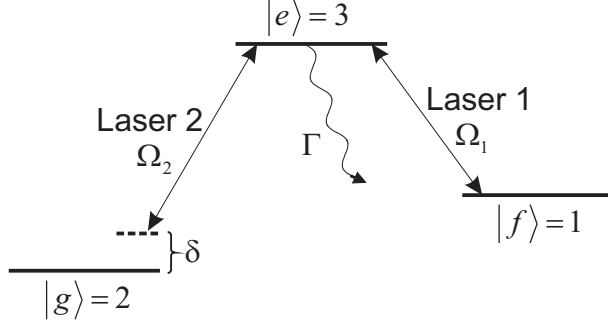


Figure 5: Level scheme for the master equation. For notational purposes, all levels are identified with an index 1 to 3.

lasers. We consider only the case where laser 1 is kept on resonance and laser 2 has a detuning δ (see Fig.). Identifying the levels $|f\rangle$, $|g\rangle$, $|e\rangle$ with the indices 1, 2, 3, respectively, the master equation reads,

$$\begin{aligned} \frac{d\rho}{dt} = & -i\delta [\sigma^{22}, \rho] - \frac{i}{2} \sum_{k=1}^2 \Omega_k [\sigma_-^{3k} + \sigma_+^{3k}, \rho] \\ & - \frac{1}{2} \Gamma (\sigma_+^{33} \cdot \sigma_-^{33} \cdot \rho + \rho \cdot \sigma_+^{33} \cdot \sigma_-^{33}) \\ & + \frac{1}{2} \gamma (2\sigma^{22} \cdot \rho \cdot \sigma^{22} - \sigma^{22} \cdot \rho - \rho \cdot \sigma^{22}), \end{aligned}$$

where ρ is the density matrix, $\Omega_{1,2}$ are the Rabi frequencies, Γ is the spontaneous decay width of the excited level $|e\rangle$, and γ is the relative linewidth of the two Raman lasers. The matrices σ_-^{rs} and σ_+^{rs} are ladder operators and each is the transpose of the other. As an example,

$$\sigma_-^{32} = \begin{pmatrix} 0 & 0 & 0 \\ 0 & 0 & 0 \\ 0 & 1 & 0 \end{pmatrix}.$$

A3. Multi-band model

In order to take into account effects of the optical lattice on the dynamics of the molecules, we use a multi-band model. In addition to the three internal states of the molecule $|f\rangle$, $|e\rangle$ and $|g\rangle$, external degrees of freedom are introduced in terms of Bloch bands (see Fig. 6). The Bloch

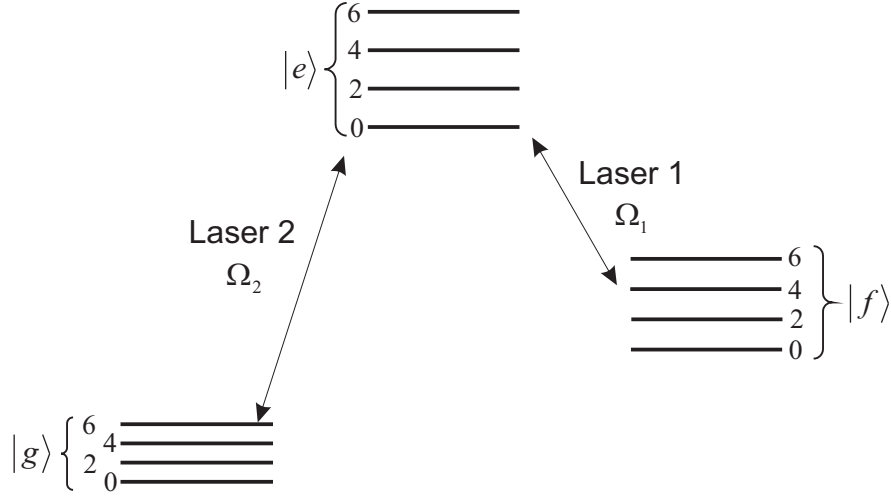


Figure 6: Multi-band model. The three molecular levels $|f\rangle$, $|e\rangle$ and $|g\rangle$ obtain a substructure due to Bloch bands of the optical lattice. We restrict the model to the 4 lowest Bloch bands with even symmetry (band index $n = 0, 2, 4, 6$).

band structure of each internal level depends on the respective lattice depth. For simplicity, we assume each molecule to be localized at a particular lattice site and its spatial wavepacket to be described by a coherent superposition of Wannier functions of the bands. The Raman lasers couple all bands of different internal states, according to the respective wavefunction overlaps. Since the initial wavepackets of the Feshbach molecules are symmetric, only even bands will be populated. We restrict our calculations to the four lowest Bloch bands with even symmetry, corresponding to the band indices $n = 0, 2, 4, 6$. The dynamics in each of the three lattice directions is then given by a 12-level model, which can be solved in terms of a master equation (see Section A2) or a Schrödinger equation (18), neglecting laser phase fluctuations. In order to treat tunneling from one lattice site to a neighboring one, we introduce a lattice site decay rate for each band. These decay rates are chosen to match the expected tunneling rate for each band and are slightly adjusted for a better fit. We note that the results of the model calculations are essentially independent of the excited state lattice depth, which is not well known.